Copyright Warning & Restrictions

The copyright law of the United States (Title 17, United States Code) governs the making of photocopies or other reproductions of copyrighted material.

Under certain conditions specified in the law, libraries and archives are authorized to furnish a photocopy or other reproduction. One of these specified conditions is that the photocopy or reproduction is not to be "used for any purpose other than private study, scholarship, or research." If a, user makes a request for, or later uses, a photocopy or reproduction for purposes in excess of "fair use" that user may be liable for copyright infringement,

This institution reserves the right to refuse to accept a copying order if, in its judgment, fulfillment of the order would involve violation of copyright law.

Please Note: The author retains the copyright while the New Jersey Institute of Technology reserves the right to distribute this thesis or dissertation

Printing note: If you do not wish to print this page, then select "Pages from: first page # to: last page #" on the print dialog screen

ABSTRACT
An Analysis of a Custom Expanding Total Femoral Prosthesis
with a Rotating Hinge Knee

by
RamaRao V. Gundlapalli

Osteosarcoma is the most common malignant bone tumor in the pediatric age group. This thesis presents the analysis of a total femoral prosthesis implanted in a 9 year old black male. The design includes a bipolar, expanding mid-shaft component, and a rotating hinge knee used in the reconstruction of the patient's right lower limb after surgical resection of the femur. The areas being analyzed are (i) the trochanteric attachment, (ii) the expanding component, and (iii) the rotating hinge knee. The stresses acting on the cables reconnecting the greater and lesser trochanter were determined for bipedal stance, single-legged stance, stance phase of gait, running and they were calculated to be 0.5 MPa, 17 MPa, 23 MPa and 51 MPa respectively. On comparing these stresses to the fatigue data for stainless steel cables, it is estimated that the cables will last for 10^8 cycles The expanding component cross-pin was analyzed to experience loads of up to three times the body weight. The maximum stress required for failure is 275 MPa at 10^7 cycles. The cross-pin is not expected to fail in fatigue. The cylindrical bearing surfaces in the rotating hinge knee experience contact stresses of 11 MPa, which is higher than the maximum stress under fatigue loading of polyethylene. The polyethylene bearing component will need to be replaced at about 10^4 cycles. Rotating knee hinge-pin component was analyzed in bending and shear, the low stresses (100 MPa and 11 MPa respectively) on the pin would give a working life of more than 10^7 cycles. The carriage-pin experiences a maximum bending stress of 98.16 MPa which is less than 50% of the maximum stress required for the titanium alloy to fail at 10^7 cycles.

AN ANALYSIS OF A CUSTOM EXPANDING TOTAL FEMORAL PROSTHESIS WITH A ROTATING HINGE KNEE

by
RamaRao V. Gundlapalli

A Thesis
Submitted to the Faculty of
New Jersey Institute of Technology
in Partial Fulfillment of the Requirements for the Degree of
Master of Science in Biomedical Engineering

Biomedical Engineering Committee

October 1993

APPROVAL PAGE

An Analysis of a
Custom Expanding Total Femoral
Prosthesis with a Rotating Hinge Knee

by
RamaRao V. Gundlapalli

Dr. Clarence W. Mayott, Thesis Adviser — Date
Assistant Professor of Mechanical Engineering, NJIT

Dr. Mark C. Zimmerman, Committee Member — Date
Assistant Professor and Co-Director,
Laboratories for Orthopaedic Research, UMDNJ

Dr. J. Russell Parsons, Committee Member — Date
Associate Professor and Director,
Laboratories for Orthopaedic Research, UMDNJ

Dr. Joseph Benevenia, Committee Member — Date
Assistant Professor and Chief,
Section of Musculoskeletal Oncology,
Department of Orthopaedics, UMDNJ

BIOGRAPHICAL SKETCH

Author: RamaRao V. Gundlapalli

Degree: Master of Science Biomedical Engineering

Date: October 1993

Undergraduate and Graduate Education:

- Master of Science in Biomedical Engineering,
  New Jersey Institute of Technology, Newark, NJ, 1993
- Bachelor of Science in Mechanical Engineering,
  Madurai-Kamaraj University, Madurai, India, 1991

Major: Biomedical Engineering

Presentations and Publications:

Kim D, Lee CK, **Gundlapalli RV**, Parsons JR; Spinous processes, Paraspinal Muscles, and Muscle Fascia Affect the Sagittal Plane Stiffness of the Lumbo-Sacral Spine. *International Society for Study of the Lumbar Spine*, Marseilles, France, June 1993.

Benevenia J, **Gundlapalli RV**, Pappas M, Kadaba MP, Zimmerman MC; An Expandable Total Femur for Limb Salvage: Design, Clinical Results and Gait Analysis. IEEE, *19th Annual Northeast Bioengineering Conference*, Newark, New Jersey, March 1993.

Lee CK, Zimmerman MC, McGinley S, Kim D, Closkey R, **Gundlapalli RV**; The Role of Paraspinal Musculature in Spinal Stability: A Biomechanical Analysis. Presented at the *New Jersey Academy of Orthopaedic Surgeons*, New Brunswick, New Jersey, October 1992.

This thesis is dedicated to
All Musculoskeletal Oncology Patients

ACKNOWLEDGMENT

As I submit my Master's Thesis, I would like to look back and acknowledge the people who have helped me to reach my goal.

First of all I would like to thank my committee members for their guidance, support and encouragement. Dr. Clarence W. Mayott has given me good advice and guidance for the presentation of my project work. Dr. Mark C. Zimmerman has been a constant source of support throughout my work at the Laboratories for Orthopaedic Research, UMDNJ. As the Director of this lab, Dr. John R. Parsons has always given me a broad prospective on research and writing that helped me in my work. As the attending surgeon, Dr. Joseph Benevenia has played a central role in this project for both design and execution. As a committee member he has always added another dimension to my thinking and work.

I owe a debt of gratitude to NJIT, especially the Biomedical Engineering Program. From the day I joined this program, Dr. David Kristol has given me his support and backing.

For a graduate student, funding and finances are important matters. I would like to acknowledge the Physics Department @ NJIT for awarding me a Teaching Assistantship during my first year here and then the Orthopaedic Labs and the Biomedical Engineering program for supporting me as an Research Assistant during my second year.

During my work and study here, I have come across many people who have helped my project, Thomas Poandl, Alecia Marcantonio, Denise Perez and all the members of the Laboratories for Orthopaedic Research, UMDNJ; Dr. Pappas and George Makris of Endotec Inc., NJ; Dr. Kadaba and H.R. Ramakrishnan of the Gait Analysis laboratory, Helen Hayes Hospital, NY.

I would like to acknowledge the co-operation shown by the patient and his family towards this study.

I would also like to acknowledge "His" blessings, family, friends and colleagues who believed that I should get a good education and encouraged me to go out and get it even though it is miles away from home.

TABLE OF CONTENTS

Chapter Page

LIST OF FIGURES

Figure Page

LIST OF TABLES

Table Page

1 INTRODUCTION

1.1 Expanding Prostheses & Total Femoral Replacements

Osteosarcoma is the most common malignant bone tumor in the pediatric age group. Improved diagnostic methods and the understanding of malignant bone tumors have increased the use of limb-sparing procedures against treatment by ablation. In order to retain the integrity of the limb following resection in pediatric age groups, several surgical procedures have been proposed (29, 41, 45, 66).

A child's skeleton grows by three-dimensional remodeling of the bones. This poses additional problems in surgical intervention to those encountered in the adult. For tumors in the major bones of a growing child, an expandable or lengthening prosthesis is a very useful alternative to amputation (8). The design and indications for use of an expanding prosthesis are listed below (42, 60, 71).

(i) Design an extension mechanism that will provide the required increase in length,

(ii) Incorporate this mechanism in a major bone that would offer the possibility of serving as either a temporary or a permanent prosthesis,

(iii) Design a means of fixation to accommodate continuing growth of the unaffected bone,

(iv) Design such a prosthesis with its surgical procedure so that if a mechanical or biological failure were to occur, a salvage operation would be possible. This procedure should result in no more mutilation that what an initial amputation would have caused.

The first expanding prosthesis was reported in 1976 by Scales *et al.* (60) who used an expanding component in either the proximal or distal femoral regions to achieve the required lengthening. The lengthening was based on the worm gear. This was judged to be the best method since it would not collapse with increasing loads. Scales in 1982 helped design an expanding prosthesis using a ball bearing mechanism made of titanium alloy. Titanium was chosen to reduce potential fretting or corrosion. The lengthening would depend on the size and number of the metal balls inserted into the extending component, FIGURE 1.

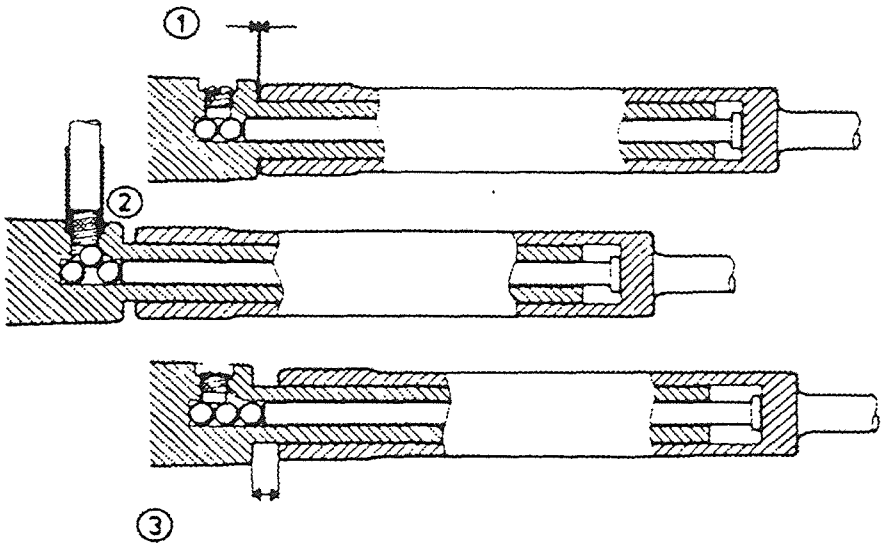

FIGURE 1 Schematic showing the Ball Bearing expanding mechanism. Step 1 shows the prosthesis, step 2 shows the metal ball being inserted, and step 3 shows the expanded prosthesis, (60).

Keanan and Lewis (37, 38) introduced an expanding component based on the Jacob's chuck screw mechanism that can be used to contract as well as expand. Reduction is necessary in extreme cases of neurovascular problems developed during the lengthening process. There have also been reported

prototype models of expanding components using the magnetic and electric motors developed by a research team in Netherlands (68).

Spires *et al.* (59, 60) conducted a biomechanical analysis of an expanding proximal femur (chuck key type) under various load and length conditions approximating the *in vivo* conditions. It was found that there were no significant seizing or galling of the titanium alloy as would be expected. They also concluded that there was no significant wear of the threads after 6 million cycles. These prostheses have been used for different kinds of resections of the long bones.

If the location of the tumor is such that there is not enough bone stock to implant either a proximal or distal expanding component, the option of a total bone replacement may be considered. Marcove *et al.* (47, 48) presented a report of 19 patients who underwent total femoral replacements due to the size or position of the tumor. All of their prostheses included a hinge knee for stability at the joint. This would provide a functional but weak limb. Their patients ranged in age from 11 to 65. Of the 19 patients, the success rate was 74%. Present and Kuschner (57) reported a total femoral prosthesis with a 35 year followup with no significant complications. The prosthesis was made of vitallium with a hinge knee joint. The patient eventually opted for a hip disarticulation. Steinbrink *et al.* (67) had 32 cases of total femurs out of which a majority were revision surgeries and only four of these patients were suffering from primary bone tumors. Nerubay *et al.* (53) had 19 patients with a total femoral prosthesis made of stainless steel and the hip joint similar to that of the Thompson prosthesis. They had a flattened section below the femoral head with perforations for possible trochanteric attachment. This kind of prosthesis did not allow for knee motion. Post-operatively they had 7 excellent, 9 good, 1 fair, and 2 poor results.

None of these cases were expanding to compensate for limb length inequality, largely due to the fact that the patients were adults or were skeletally mature. No biomechanical studies have been reported to support the success of a total expandable femoral implant.

1.2 Hinge Knee Replacement

A common method to treat unstable knees with considerable bone and soft tissue loss is to use a hinged prosthesis. One of the earlier designs was that of the Walldius (70) in the early 1950s. Similar designs such as the Stanmore (43), Caviar Madriporic knee prosthesis (39) and the GEUPAR (18, 17) were introduced during the 1970s. The long term results of these prostheses were not satisfactory (5, 17, 30, 33, 70) due to the high rates of loosening and difficulty in revision surgery which led to the virtual disuse of all hinged prostheses.

Newer designs were introduced to overcome the shortfalls of their predecessors. Theses designs include Attenborough (6), spherocentric (36), Herbert (52), Seehan (64), St. George (22), Noiles (64), Lacey, GT-Prosthesis (9), Finn knee (23), and the Kinematic rotating hinge knee (69) implants. All of the above implants were introduced with metal-polyethylene bearing surfaces and rotations about axes other than that of flexion/extension.

The Noiles hinged prosthesis was introduced as an implant which would reduce the shear and the tensile loading on the bone-cement interface. This would reduce the complications of loosening. The components include a cemented femoral stem that articulates through a hinge pin with an uncemented tibial stem. This stem fits in a polyethylene sleeve which would be cemented in the tibia. This design would allow for a 20 degree arc of axial motion as well as flexion and extension. Four studies on the Noiles

prosthesis were reported, two by Accardo *et al.* (2, 3) and one each by Holt (28) and Shindell *et al.* (65). Accardo reported a total of 119 knees in a span of 3 years with only 2 failures. Holt reported a good success rate in his 27 knees with only one failure due to infection. Contrary to Accardo and Holt, Shindell reported a study of 18 knees with success rates of only 56%. The failures were attributed to prostheses subsiding into the tibial bone and loosening at the bone cement interface.

The Attenborough total knee replacement (6) is a compromise between the restrained hinges and the unconnected surface or condylar prostheses. It is a two piece prosthesis with the normal gliding movements of flexion and extension and has a stabilizing rod between the femoral and tibial components which allows some lateral and rotational laxity. The components are designed such that when either rotation or lateral movements occur the joint opens and gradually tightens the soft tissue rather than a sudden polyethylene block which would loosen the implant. Between 1973 and 1977, Attenborough reported on a total of 245 knees and after 1977 a revised design was used in 83 knees. A total of 38 knees were lost either due to death or arthrodesis and the rest were judged as successful. Attenborough concluded that this prosthesis could be successfully used in patients where condylar prostheses would fail due to lack of inherent stability.

The Sheehan prosthesis (64) has two separate bearing surfaces with a gap for the stabilizing stud of the tibial component which interlocks between the femoral bearing surfaces and engages the inner radius thus ensuring the stability of the joint. The external surface of the femoral component has a curvature simulating that of the normal knee. The internal femoral radius engages in the groove of the expandable tibial stud. It simulates cruciate stability by preventing anterior and posterior movement but at the same time

allows a combination of sliding and rolling between the bearings. This allows for 2-3 degrees of valgus-varus motion to a maximum of 6-7 degrees when the knee is semiflexed. When the knee is flexed to about 30 degrees, it allows approximately 20 degrees of axial rotation. Over 4000 of these prostheses have been implanted since its introduction and Sheehan has reported on his initial 157 patients (64). They were evaluated for post-operative pain and 80.9% showed no pain, 16% had mild pain, 2.3% had significant pain and 2.3% had severe pain. There were 7 patients with mechanical complications of which 4 had detached tibial components, one had the tibial stud fractured, one had bone resorption of the lower femoral condyles and upper tibia and one needed a realignment of the femoral component.

Walker *et al.* (69) designed the Kinematic rotating hinge knee to overcome the disadvantages of regular hinged knees with axial rotation coupled with flexion/extension. The design addresses the following questions:

(i) In flexion/extension, how is hyperextension prevented and what is the range of flexion before impingement?

(ii) In rotation of the femur about the tibial axis, is the prosthesis unrestricted?

(iii) To what degree is the valgus-varus alignment restricted?

(iv) Is there provision for replacement of the patello-femoral joint?

(v) Is bone removed primarily from the ends of the femur and tibia or is femoral intercondylar bone also removed?

The prosthesis to be designed for such specifications needed to be more complex in nature and required considerable analysis and testing prior to its

use (19, 20, 61, 69). The prosthesis consisted of seven components, the metallic femoral component, two polyethylene bushings inserted into the femoral flanges, a polyethylene tibial plug accepting the metal tibial bearing component, a metal axle passing through the bushings and the hole in the tibial bearing component. The axle was locked in place with a snap-in axle lock that also served as an extension stop. The polyethylene bushings were cyclically tested for their wear characteristics. A load of 1960 N was placed on the prosthesis on a material testing machine and flexed in an arc of 30°. Water was used as a lubricant. A maximum wear of 0.23 mm was found after five million cycles (corresponding to about 5 years of usage). The load was then moved off-center by 24 mm and the same tests were performed, this time the polyethylene bushing on the side of the load deformed. The rotating hinge controls all linear motion except for distraction. This prevented the tensile forces acting across the joint. Rotation about the tibial axis was allowed and was controlled by the conforming geometry of the femoral condyles which also helped create a soft stop during rotation. The cylindrical bearing surfaces were designed to carry all the force by area contact rather than point or line contact and the metal rod resisted the shearing forces. Of the 200 implants made between 1978 and 1980, only five failed, mainly due to misalignment and lack of tibial support resulting in the fracture of the proximal tibia.

The Finn Knee design consisted of a rotating hinge. The femoral component articulated with the tibial component through an axle-and-yoke mechanism. The femoral component allowed up to 5 degrees of valgus alignment and approximates the surface geometry of the distal femur. The femoral component accepted an axle which rotated on ultra high molecular weight polyethylene (UHMWPe) bushings. The axle is fixed using a

UHMWPe pin. The tibial component is stemmed to accept the rotating yoke in an UHMWPe bushing. A weight bearing interface through a tibial rotating bearing made of UHMWPe creates the articulation. The prosthesis is designed either to be press-fitted or cemented using polymethylmethacrylate (PMMA). The patella is resurfaced using a UHMWPe patellar component. The kinematics of the prosthesis allows for a freedom of flexion to 135°; extension of 0°; internal-external rotation of 20°. In extension, the weight is shared throughout the composite structure and not by the axle alone. In flexion, the load is shared by the axle and yoke mechanism and by the tibial bearings only. This design provides for congruent articulating surfaces between the femoral and tibial components. Congruent geometry provides for even distribution of weight bearing forces through surface contact rather than point contact. The femoral component has a deep groove for optimal patellar tracking. A clinical study done by Finn (23) on 23 knees (between 1989-1991) showed no failure of fixation or joint stability or even of patellar-femoral tracking problems. One patient was revised due to a pathologic fracture, 3 patients had skin necrosis, and one patient had developed an infection and an amputation was required.

Kester *et al.* (40) and Kagan (35) evaluated the mechanical failure modalities of rotating hinge knee prostheses. The most common device failure was its progressive subsidence due to the compressive forces on the knee (7). Gall wear of the polyethylene components was another significant cause. Implant loosening and instability was the cause of failure in approximately 10% of the cases reviewed. Postoperative roentgenographic analysis revealed prosthetic migration, stress induced remodeling and loss of condylar bone.

1.3 Expanding Total Femoral Prostheses with Hinge Knee

This thesis presents a novel design of a total femoral prosthesis implanted in a 9 year old black male. The design includes a bipolar, expanding mid-shaft component, and a rotating hinge knee used in the reconstruction of the patient's right lower limb after surgical resection of the femur. The following factors led to the design of this prosthesis:

(i) Complete removal of the femur was necessary for local tumor control.

(ii) The patient was skeletally immature with an expected longitudinal growth of seven to ten centimeters.

(iii) An arthroplasty (hip and knee joint replacement) would allow the most naturally functional and cosmetically appealing limb.

It is the aim of this thesis to critically examine this total femur design; looking in detail at the areas of potential long term failures.

2 MATERIALS AND METHODS

2.1 The Prosthesis

TABLE 1 Table showing the areas of study of the device design

	FEATURE	AREA OF INTEREST
1.	Material	(a) Ti6Al4V alloy (b) TiN coating
2.	Trochanteric attachment	(a) Failure of bone/resorption (b) Failure of wire
3.	Expanding mid-shaft	(a) Shear in Cross-pin
4.	Mid-shaft and knee varus/valgus attachment	(a) Shear in Cross-pin
5.	Rotating hinge knee	(a) Cylindrical bearing surfaces (contact stress and wear) (b) Hinge pin (shear/bending) (c) Hinge pin bushing (PE Vs. metal) (d) Metal rod (knee axle) (i) Shear at fillet (ii) Moment on the rod (e) PE tibial insert (wear and fatigue)

The Total Expanding Femoral prosthesis is a combination of three elements a total hip, an expanding mid-shaft and a rotating hinge knee. The prosthesis is essentially made of titanium alloy (Ti6Al4V) with Ultra High Molecular Weight Polyethylene (UHMWPe) bearing surfaces. The device design is shown in FIGURE 2. The key design features are numbered on the illustration, tabulated in Table 1, and described below.

1) Bipolar Acetabulum with UHMWPe cup is recommended in children because replacement of the polyethylene articulating liner is a relatively simple procedure and because acetabular growth is not inhibited.

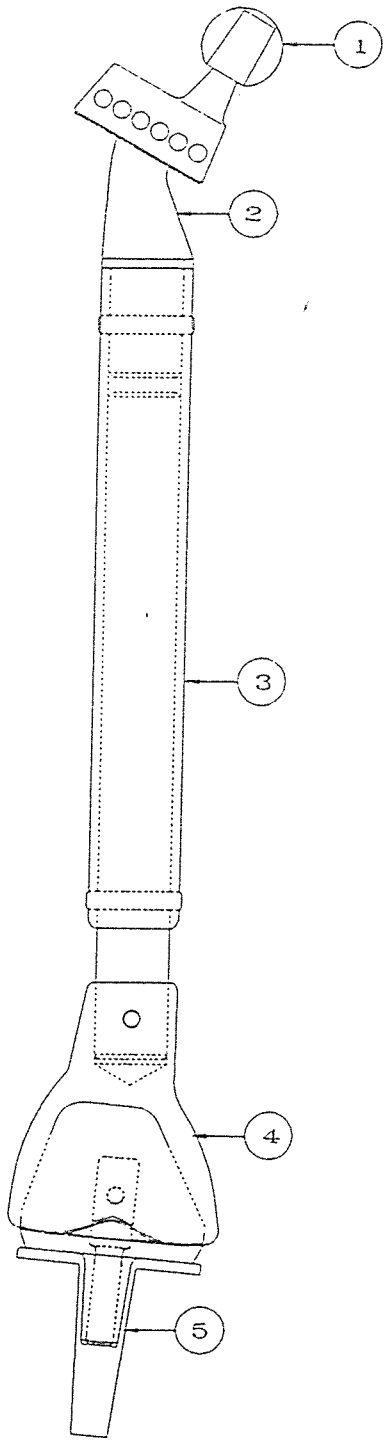

FIGURE 2 The complete device design with the key features numbered.

2) The greater trochanter can be cabled around the prosthesis in order to maintain abduction and to provide proximal stability. The muscle would maintain the vascularity of the bone. A porous surface on the prosthesis would allow bone ingrowth and stability.

3) Total bone growth is determined using tables from (4). The expanding midshaft was designed to provide the required lengthening. A telescoping tube-in-tube with a cross pin was the design with the least micromotion and wear. Spacing between cross pins was 9.5 mm, providing a potential total length increase of 133 mm.

4) The sacrifice of ligaments about the knee results in global instability that can only be restored by a constrained knee design. This design provides for flexion-extension, axial rotation and pistoning of the tibial shaft within an UHMWPe sleeve during flexion-extension only.

5) The proximal tibial epiphysis was salvaged and a non-cemented, modular, press-fit, porous coated tibial plateau was inserted (51). A UHMWPe polyethylene insert was used for the hinged knee articulation.

6) The prosthesis was made of a titanium alloy (Ti 6Al 4V) because of its excellent mechanical fatigue properties, resistance to corrosion, and biocompatability. Biocompatability and wear resistance are further enhanced by a surface nitriding process which increases surface hardness.

The trochanteric attachment was made by using multifilament stainless steel cables (1.6 millimeters in diameter) to cuff the greater and part of the lesser trochanter to the proximal stem of the prosthesis. Although proximal holes were designed for this purpose, it was decided during surgery that cabling the bone stock to the stem would suffice. Three loops of the cable were used to hold the bone in place. A porous coating was provided proximally so that the bone would grow into the stem and allow for better fixation. The angle of the abductor muscle force was determined using force vector diagrams; the abductor forces for different scenarios were determined using free body diagrams; the cable tension on the attachment was also analyzed using free body diagrams

The expanding component was designed to minimize the micromotion and wear debris experienced by other expanding prosthesis designs. The expansion would be achieved by removing the cross-pin and separating the compound tubes with the help of a custom made distracter, FIGURE 3. Once the required lengthening is achieved, the cross-pin would again be inserted in place. The cross-pin is designed to take the axial and shearing loads on the mid-shaft. The shearing load on the cross-pin was determined from force plate data recorded during gait analysis. The load is determined by vector analysis.

As mentioned, a hinged knee is used in the reconstruction of knees where there is loss of soft tissue and ligaments. In this patient most of the extensor mechanism was removed and the only way to maintain knee stability was to use a rotating hinged knee. This knee is a custom design and contains features from the Kinematic hinge knee and the Finn knee. This knee allows for flexion of 130° and extension of 0°. It also provides for an axial rotation of ±10°; FIGURE 4.

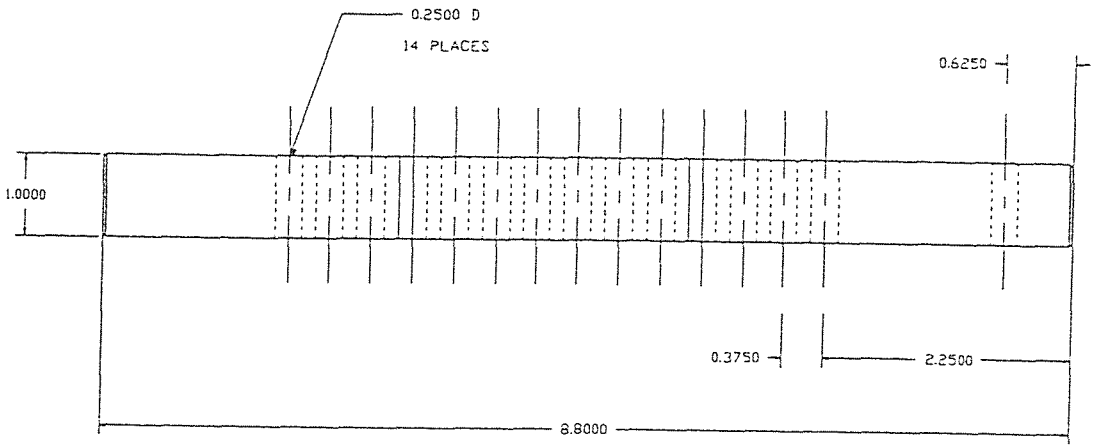

FIGURE 3 Schematic of the expanding tube-in-tube component showing the maximum length and the length increase per cross-pin shift in inches.

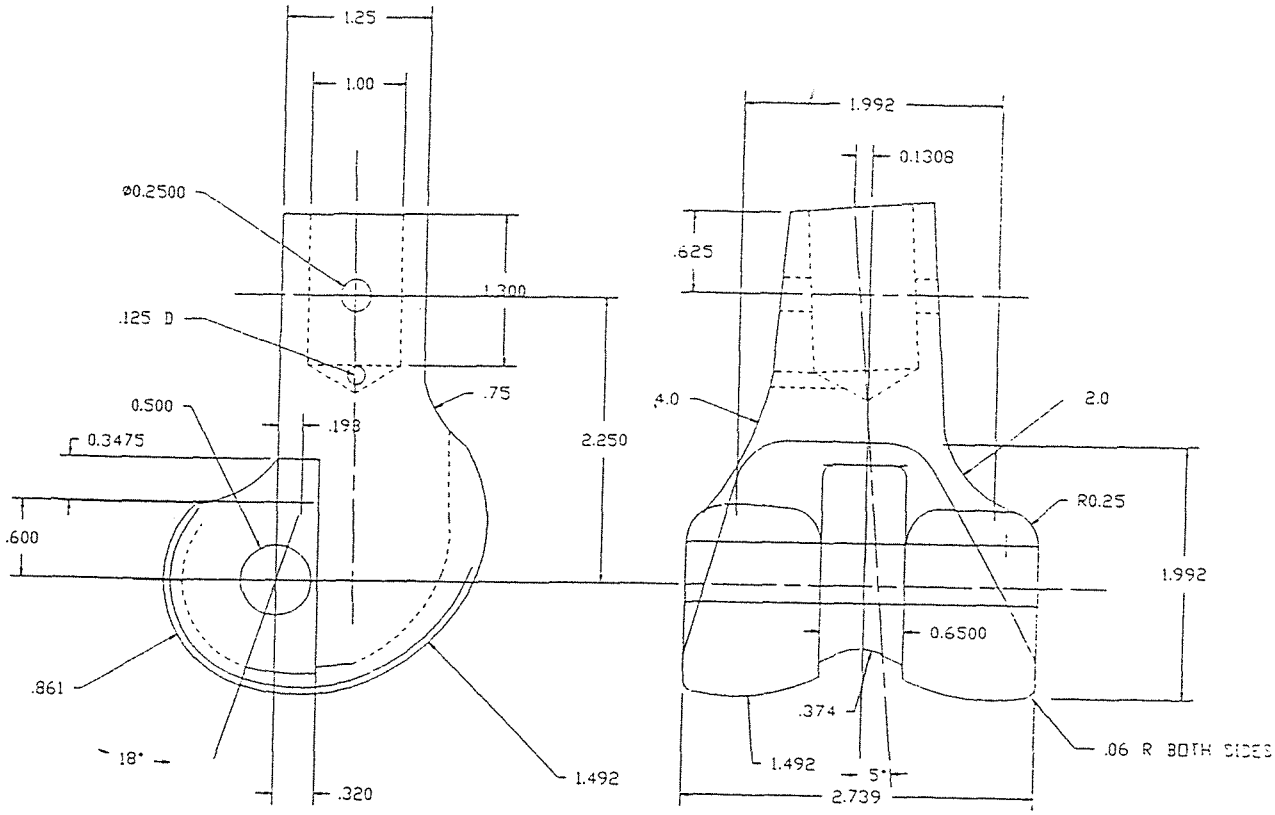

FIGURE 4 Distal femoral component of the prosthesis showing the anterior-posterior and the lateral views. Major dimensions are indicated in inches.

The cylindrical bearing surfaces of the knee were analyzed using data and equations form Seely and Smith (62). The principal stresses are determined from non-dimensional values and the contact area from the geometry of the knee. The hinge pin was analyzed as a free body diagram assuming that the pin is supported on UHMWPe. The moment on the carriage-pin was also determined using free body diagrams for the worst case scenario. The wear on the polyethylene components were derived from previously published data.

The Ti6V4Al alloy properties are enhanced by nitriding the surface using the vapor deposition method described by Bernard *et al.* (13). The alloy is initially coated to a thickness of 10 microns and then polished to a 0.04 micron finish. This nitriding reduces the wear amount to two-thirds of that produced by its cobalt-chrome counterpart. This is mainly due to the TiN coating being resistant to transfer film formation (34). The wear of the metal-polyethylene surfaces were derived from pin-on-disc experiments done by Jacobson *et al.* (34).

2.2 Surgical Procedure

The patient underwent a nine-hour operation where the right femur was resected. There was a subtotal resection of his quadriceps mechanism including the vastus medialis, vastus intermedius, and vastus lateralis (partial). The proximal portion of the femur was carefully osteotomized in the sagittal plane, leaving the greater trochanter intact with the gluteus medius and the vastus lateralis sling attached to it. The lesser trochanter was left with its psoas tendon and calcar attached. The patella along with a partial extensor mechanism was retained.

The prosthesis was implanted. The extending component was assembled so that there was one centimeter increase in length compared to

the contralateral limb. The rotating hinge knee was assembled along with its UHMWPe bearings. The porous coated tibial plateau was press-fitted into the proximal tibia. The carriage pin of the knee component was inserted into the tibial plateau with a polyethylene bearing. The greater and lesser trochanter were cabled around the proximal region of the prosthesis. Due to excessive soft tissue resection a free latissimus dorsi muscle flap was provided to attain coverage.

2.3 X-Ray Measurements

All physical measurements were taken from the patient's roentgenograms. X-rays of the standing patient were taken to obtain anatomical distances between the joints and the center of gravity so that the line of action of forces through the lower limb could be determined. Supine x-rays revealed the patient's limb length discrepancies. X-rays of individual components of the prosthesis were also taken to determine the positioning of the prosthesis relative to anatomical markers. During theoretical analyses, care was taken to note that the x-rays had a 11% magnification and necessary reductions were made.

2.4 Gait Analysis

The patient underwent post-operative gait analysis at 13 months at the Gait Analysis Laboratory, Helen Hayes Hospital, NY. Pre-operative gait analysis was not done and hence not available for comparison. Thus the patients gait was compared to that of normal 9-10 year old patients.

The patient was asked to walk on a prescribed pathway which had a force plate to obtain the ground reaction forces of the patient. To determine the anatomic trajectories of the joints, markers were used. The patients gait

patterns were recorded on a computer system using infra-red cameras and an image capturing system. Foot switches were used to obtain the foot pressure pattern. Surface electrodes were placed on muscle sites to record the electromyographic data of the patient. The patient was asked to walk the pathway at normal speed and an average of three cycles was taken. Static readings were also obtained to be compared with dynamic gait.

3 RESULTS AND DISCUSSION

3.1 Abductor Attachment

Reattachment of the greater and lesser trochanter after osteotomy is still considered the best approach to regain normal lower limb activity. The gluteus medius and vastus lateralis to the greater trochanter and the psoas tendon to the lesser trochanter are the major muscle and tendon groups involved in the abduction and adduction of the lower limb. The most frequently used method of reattachment remains wiring.

The wires must be able to overcome the abductor forces counteracting the body weight. These forces usually are in the order of twice the body weight (32, 49, 50) and act in both the vertical plane and the anteroposterior plane when the hip is flexed. The anteroposterior shearing forces can reach up to four times the body weight and the muscles can produce a rotational force at the insertion points. The shearing forces can be overcome as long as there is a compressive force between the bone surfaces maintained by the cables/wires.

In this study, the greater and lesser trochanter along with their muscles groups were osteotomized along the saggital plane. The trochanters were then cuffed around the prosthesis using a 1.6 millimeter multifilament stainless steel wire (14, 15), FIGURE 8.

Three wire loops were made. One was proximal and the other two distal to the bone stock. Although there were three wire loops in the reattachment procedure, the most distal of them was used in the calculations because it would experience the maximum bending forces. This cable was at an angle of 85° from the vertical.

The trochanteric attachment was assumed to be a potential area for failure in the prosthesis and was thus systematically analyzed. There are two potential modes of failure of the attachment

(i) Failure of the bone stock by fracture-resorption and

(ii) Failure of the cable.

Assumptions

The assumptions made for the analyses were that

(i) The model is two dimensional,

(ii) The conditions were static,

(iii) The greater trochanter was assumed to take most of the force of the proximal femur,

(iv) The cables were always in tension and not in compression,

(v) There were no soft tissue tensions involved,

(vi) The most distal cable was assumed to carry all the load resulting from the abductor forces and hence was the one considered.

TABLE 2 Mass ratios of abductor muscle groups

Muscle Groups	Mass Ratios
Gluteus medius	4
Gluteus minimus	2
Tensor facia femoris	1
Gluteus maximus (anterior)	1

Since the trochanters were re-positioned, the line of action of the abductor force was calculated using published data (32, 50, 63). The four muscle groups involved in the abduction of the lower limb are the gluteus medius, gluteus minimus, tensor facia femoris and the gluteus maximus (anterior). The mass ratios of the four muscle groups are tabulated in table 2.

The force vector magnitudes are directly proportional to the mass ratio of the muscle groups (50). The direction of the line of action of the muscle groups were determined from patient x-rays. In FIGURE 5, P represents the point of insertion of the gluteus medius and the gluteus minimus; Q represents the point of insertion of the tensor facia femoris and the gluteus maximus (anterior).

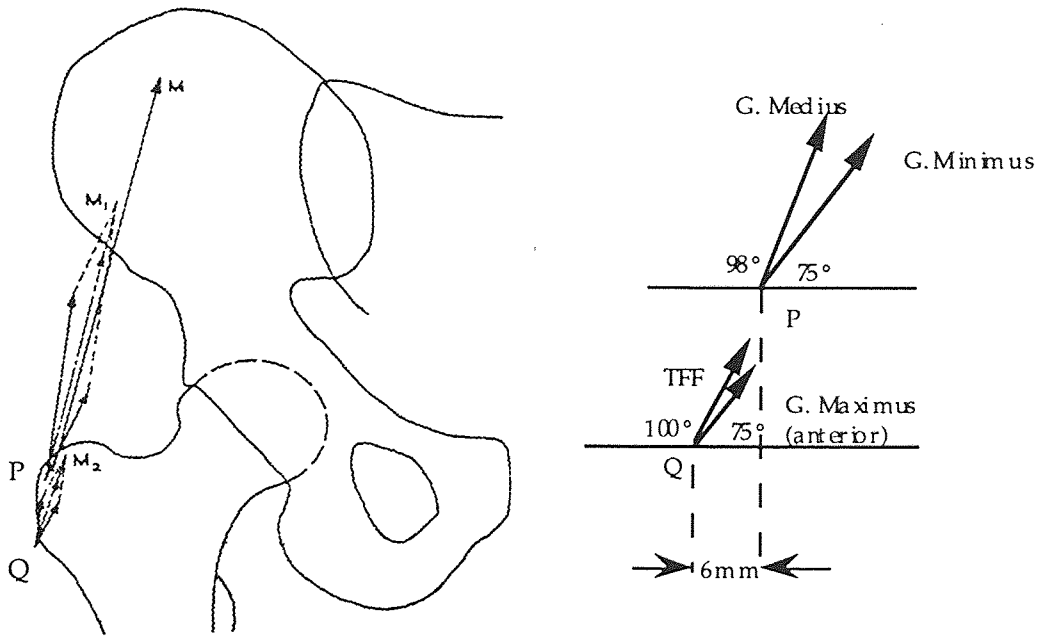

FIGURE 5 Determination of resultant abductor muscle force.

Adding the vectors, the resultant is at an angle of ø = 79.2° from the horizontal.

With the angle for the abductor force, a simple bipedal standing man and a single stance free body diagram was used to determine the abductor force and the femoral head reaction force.

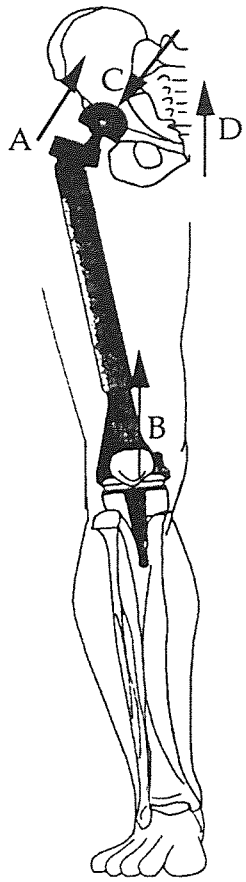

FIGURE 6 Figure of the prosthesis in place showing the anatomic points of the line of action of the various forces.

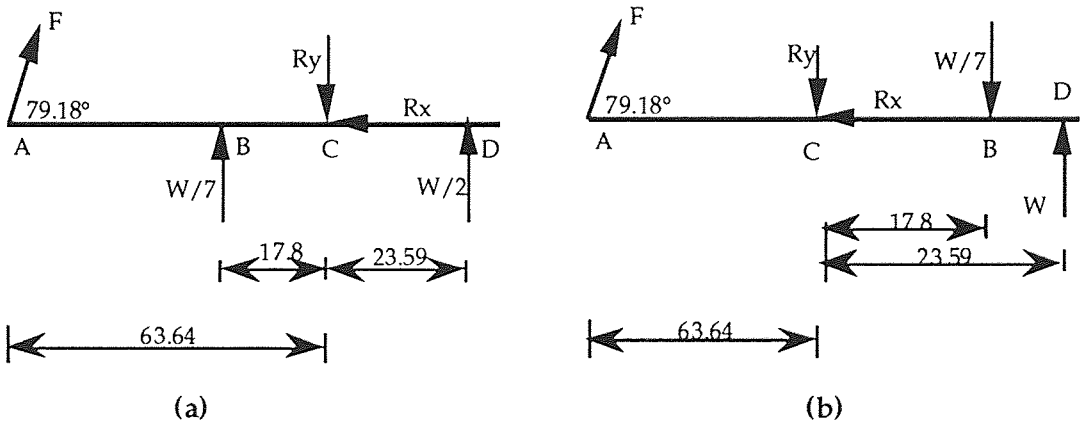

FIGURE 7a & 7b (a) Free body diagram of a bipedal standing man.
(b) Free body diagram of a single legged stance.

FIGURE 6 shows the positions of the forces acting on the affected right limb. Point A is the insertion point of the abductor muscles, point B is the reaction force due to the weight of the leg, C is the hip joint reaction force and D is the reaction force due to the weight of the body. FIGURE 7a gives the free body diagram for the bipedal stance and FIGURE 7b for a single leg stance.

Similarly, two other scenarios were considered

(i) Stance phase of gait (forces on the hip joint ≈ 2.7*Body Weight),

(ii) Patient running (forces on the hip joint ≈ 5.8*Body Weight), (16, 25, 44).

The cable tension and the reaction forces and are shown in table 3. The accompanying figure FIGURE 8 shows the greater trochanter as a free body diagram with the force vectors in place. The anatomic distances between various points are also provided. Force calculations were also made assuming that the reaction force (on the bone from the prosthesis) was a uniformly distributed load. These results are also tabulated, table 4.

TABLE 3 Abductor muscle force and distal cable tension for various patient activities

Activity	Abductor Force (N)	Force on the Femoral Head(*BW)	Cable Tension (N)
Bipedal stance	52.45	0.8	4.05
Single leg stance	986.61	2.1	137.32
Stance phase of gait	1313.67	2.7	182.85
Running	3119.27	5.8	412.64

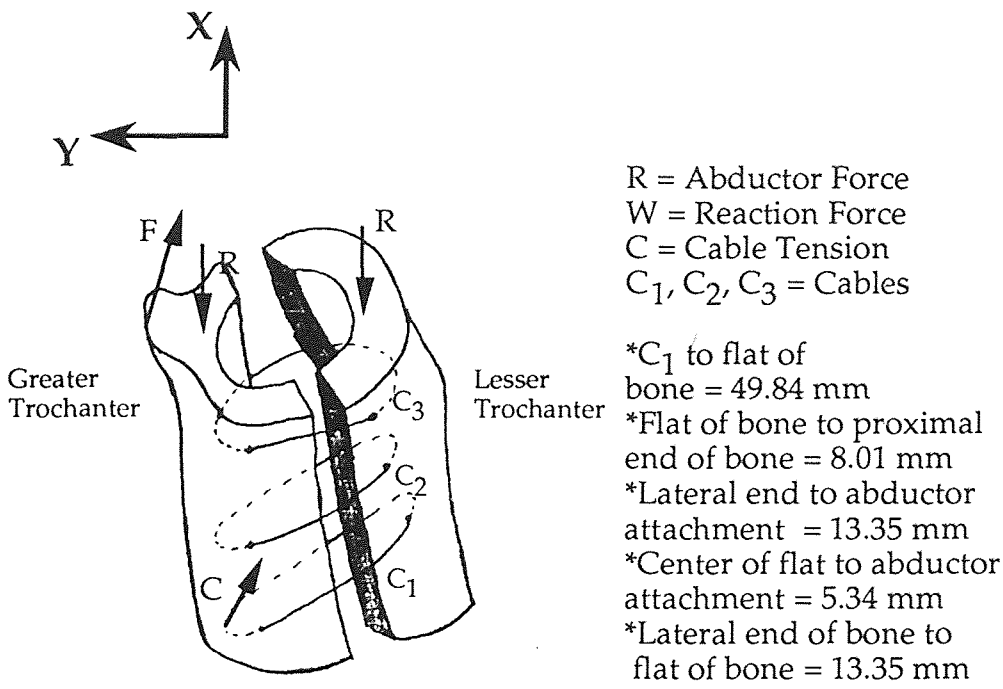

FIGURE 8 Schematic of the trochanteric cable system attachment.

TABLE 4 Force on the bone from the prosthesis assuming a single point load and a uniformly distributed load

	REACTION FORCE	
Activity	R = Single point load (N)	R = Uniformly distributed load (N/mm)
Bipedal stance	57.26	$R_X = 0.36$ $R_Y = 0.09$
Single leg stance	1123.31	$R_X = 6.86$ $R_Y = 1.22$
Stance phase of gait	1306.25	$R_X = 8.10$ $R_Y = 2.66$
Running	3348.23	$R_X = 19.5$ $R_Y = 6.51$

3.2 Expanding Component Cross-Pin

The cross-pin mentioned earlier was designed to take shear loading experienced by the mid-shaft of the prosthesis. The cross-pin was intended to be a tolerance fit across the compound tubes. This would restrict independent motion between the tubes and the cross-pin.

In order to determine quantitatively the amount of shear loading across the pin, gait analysis results were used. The force plate data provided the vertical and torque values at each point of the gait cycle, FIGURE 9.

The shearing force was obtained by vectorially adding the axial stress and the torsional shearing stress across the mid-shaft.

$$\text{Shearing force} = \text{Vertical force/area} + \text{Torque}*C/J$$

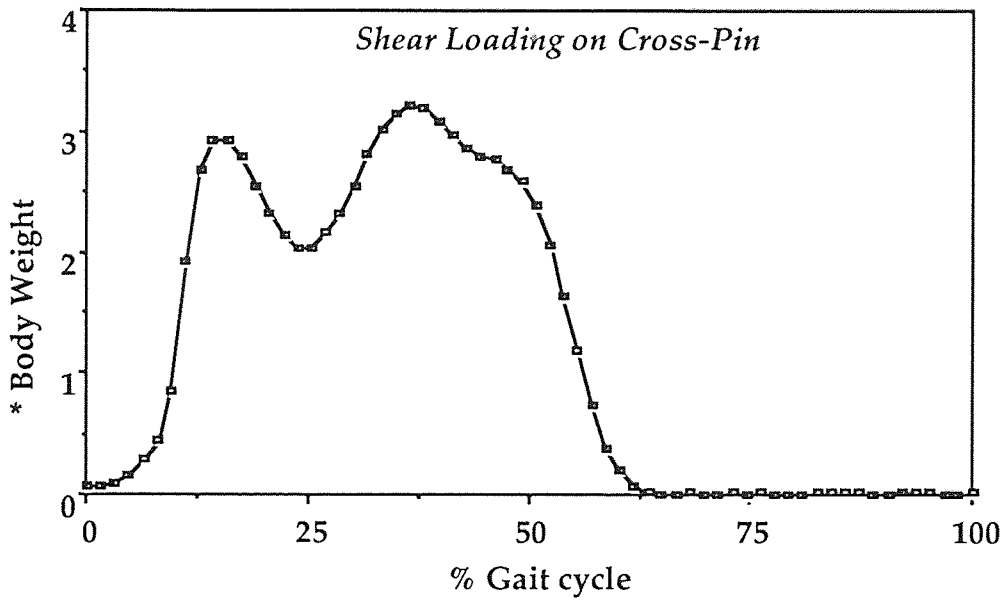

FIGURE 9 Graph of the shear loading on the expanding component cross-pin in terms of body weight. Force plate data from the gait analysis was used.

The calculated shear load is plotted in terms of body weight in FIGURE 9. The loads approach three times body weight at 35% of the gait cycle. Due to the similarity in design and function of this cross-pin with that of the pin

used in the varus-valgus attachment of the knee and the midshaft, it is assumed that the same shear loads result.

3.3 Rotating Hinge Knee

The rotating hinge knee was analyzed at three potential sites of failure. FIGURE 11 shows a schematic of the rotating hinge knee in the lateral view with the key features numbered

(1) Cylindrical bearing surfaces

(2) Hinge pin

(3) Carriage pin

3.3.1 Cylindrical Bearing Surfaces

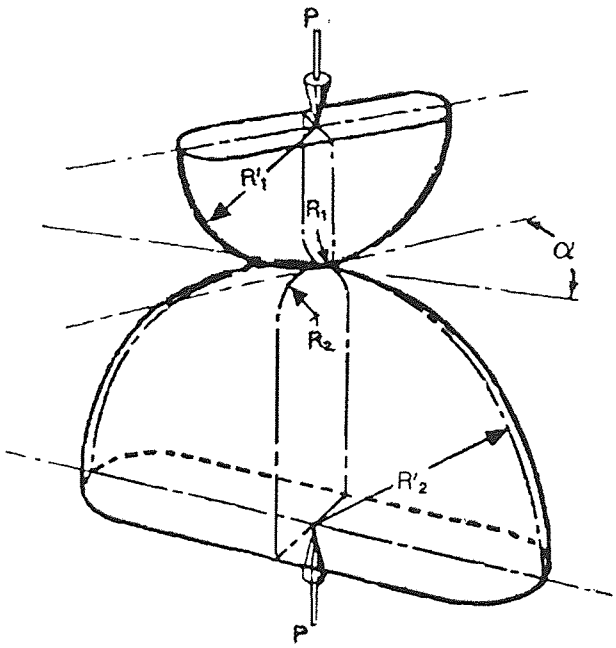

FIGURE 10 Two curved surfaces of different radii pressed against each other, (62).

The cylindrical bearing surfaces are the contact surfaces between the condyles and the UHMWPe tibial insert. The contact surfaces determine the amount

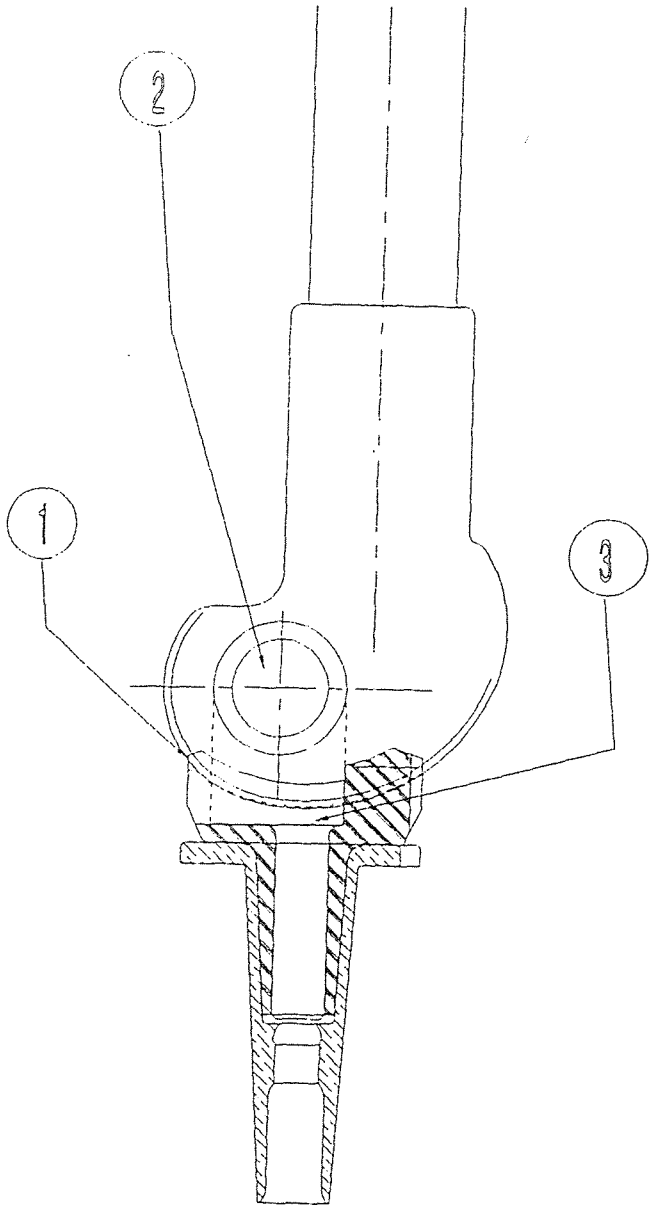

FIGURE 11 Schematic of the distal femoral prosthesis in the lateral view showing the various components as numbered in text.

of stresses experienced by the components (11, 12, 21, 31). When two incongruent bodies are in contact under the action of a compressive load, the maximum fatigue producing stress occurs under the surface. If this stress is above the fatigue strength of the material, cracks will develop under the contact surfaces resulting in pitting wear. Such wear is typically present in the tibial plateaus of knee prostheses. The equations for contact stresses were developed in Seely and Smith (62), and were modified by Pappas *et al.* (55).

Notation and meaning of terms (see FIGURE 10)

Tibial component (UHMWPe) was considered as body 1

$R_1 = R_1' = -37.78$ mm

Femoral component (Ti6Al4V alloy) was considered as body 2

$R_2 = 21.53$ mm.

$R_2' = 37.3$ mm.

Where

R_1 & R_1' = Principle radii of curvature of body 1, FIGURE 10 (assume geometric constant of B)

R_2 & R_2' = Principle radii of curvature of body 2 (assume geometric constant of A)

α = Angle between planes of minimum (or maximum) curvatures at point of contact.

P = Total force or pressure exerted by body 1 on body 2

$P = 1063.64$ N $\approx$ 3*BW

E_1, E_2 = Tensile (or compressive) moduli of elasticity for bodies 1 and 2

$E_1 = 99$ GPa

$E_2 = 0.8$ GPa

μ_1, μ_2 = Poisson's ratio for bodies 1 & 2

$\mu_1 = 0.3$

$\mu_2 = 0.25$

a = Semi-major axis of ellipse of contact

b = Semi- minor axis of ellipse of contact

Computation of Contact Stresses

As the planes of contact are parallel, the angle $\alpha = 180°$

Thus the equations for the geometric constants A & B reduces to

$$B = 1/2[(1/R_1) + (1/R_2)]$$

$$A = 1/2[(1/R_1') + (1/R_2')]$$

Solving

$A = 6.25$ mm

$B = 0.11$ mm

$B/A = 59.4276$

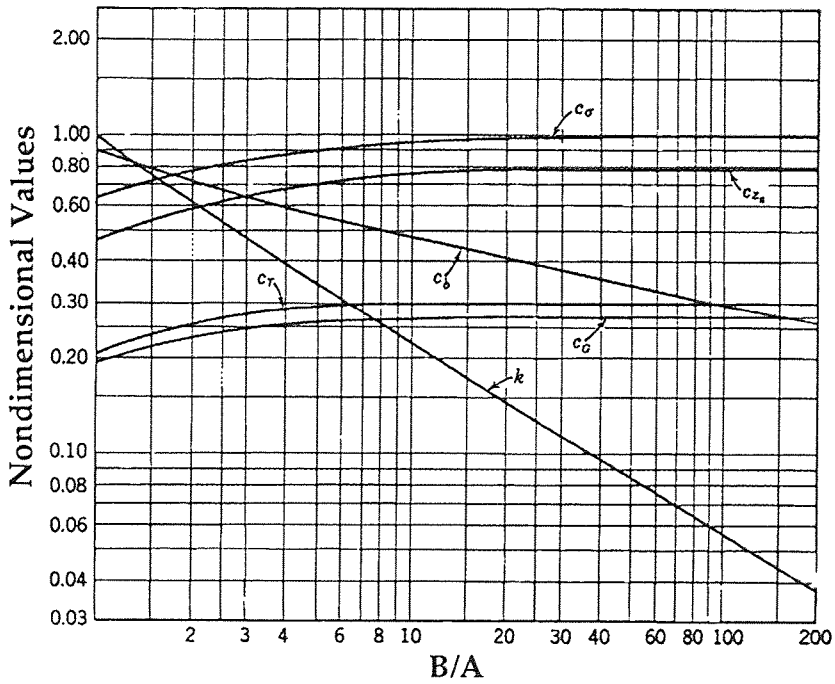

FIGURE 12 Stresses and deflections between two bodies in contact, (62).

Given the ratio of B/A, the following constants can be derived from the graphs provided in Seely (62), FIGURE 12

$k = 0.08$

$c_\tau = 0.3$

$c_G = 0.26$

$c_b = 0.34$

$c_{Z_s} = 0.79$

$c_\sigma = 1.0$

The expressions for the contact stresses are given as

Maximum principle stress $\sigma_{max} = -c_\sigma (b/\Delta)$

Maximum shearing stress $\tau_{max} = c_\tau (b/\Delta)$

Maximum octagonal shearing stress $\tau_{G_{max}} = \tau_G(b/\Delta)$

where

$$\Delta = (1/A+B)[(1-\mu_1^2)/E_1 + (1-\mu_2^2)/E_2]$$

$\Delta = 0.19$

From the expression relating B/A and k

$k = 0.075$

hence,

$k' = \sqrt{1-k^2} = 1.0$

The semi-major and minor axis were found to be of contact ellipse

$b = 2.00$ mm

$a = 26.67$ mm

Substituting the coefficients in the stress expressions

$\sigma_{max} = -10.53$ MPa

$\tau_{max} = 3.16$ MPa

$\tau_{G_{max}} = 2.74$ MPa

The depth z_S below the surface of contact of the point at which the maximum stresses τ_{max} and τ_{Gmax} occur is

$z_S = c_{z_S} b$

$z_S = 1.58$ mm

Assumptions on which solution for contact stresses are based

(i) The materials are homogenous, isotropic, and elastic and the two bodies are not necessarily made of the same material,

(ii) The dimensions at the contact patch are small relative to the principal radii,

(iii) Shape of the surfaces before and after loading are known.

3.3.2 Hinge Pin

The hinge pin allows for the flexion-extension motion of the knee. It is the pin which passes through the condyles and the carriage pin, FIGURE 13. The hinge pin was analyzed for its bending and shearing stresses using techniques from Seely (62) and Popov (56).

An assumption was made regarding the support, based on the design and position of the hinge pin. It was assumed that the pin was on a continuous UHMWPe support with a concentrated load of three times body weight acting on the center.

Computation of stresses across the hinge pin

P = Concentrated load acting on the continuous beam

P = 1063.64 N (3 * BW)

$E_{Ti6Al4V}$ = Elastic modulus of Ti6Al4V alloy = 99 GPa

E_{UHMWPe} = Elastic modulus of UHMWPe = 0.8 GPa

c = Diameter of the pin = 7.75 mm

β = Constant relating elastic moduli of metal and plastic

$\beta = 4\sqrt{E_{Ti6Al4V}/4E_{UHMWPe}}\, I = 58.12/m$

The expressions for the stresses are

Maximum Bending moment = $M_0 = P/4\beta$

$M_0 = 4.58$ Nm

Maximum Deflection = $y_0 = \beta P/2k$

$y_0 = 0.04$ mm

Maximum Bending stress = $\sigma_{max} = M_0\, c/I$

$\sigma_{max} = 0.1$ GPa

Maximum shear = $V_0 = P/2$

$V_0 = 531.82$ N

Maximum shear stress = $\tau_{max} = 11.23$ MPa

The design of the pin includes a fillet at the center, so a theoretical stress concentration factor for pure bending was taken from graphs in Seely, FIGURE 14

From the geometry of the pin

$\rho = 2.35$ mm

d = 6.2 mm

$\rho/d = 0.38$

t = 0.775

$t/\rho = 0.33$

$K_t = 1.35$

Nominal Bending stress = $\sigma_0 = \sigma_{max}/K_t$

$\sigma_0 = 74.10$ MPa

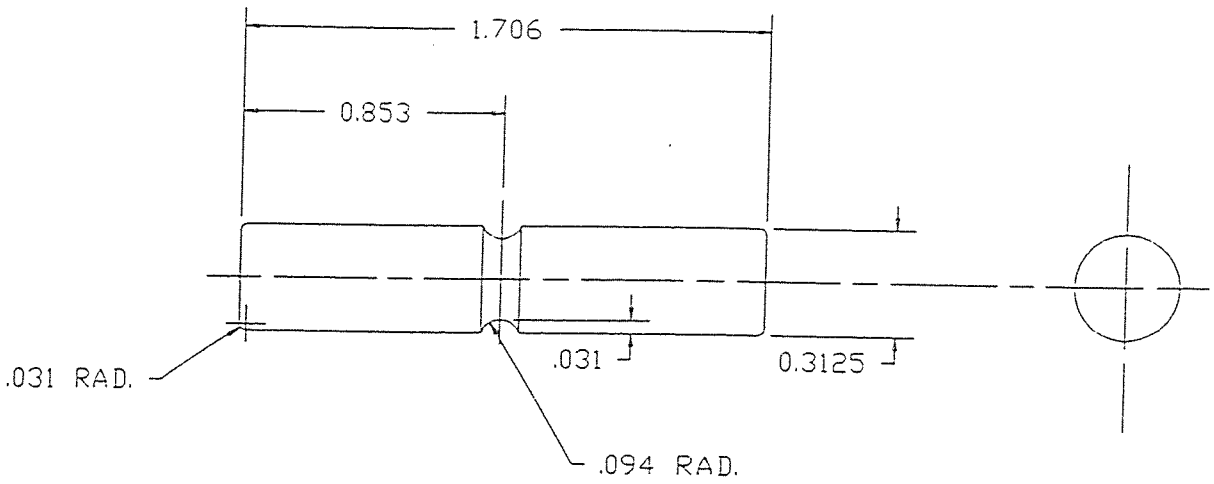

FIGURE 13 Hinge-pin component of the kinematic rotating hinge knee.

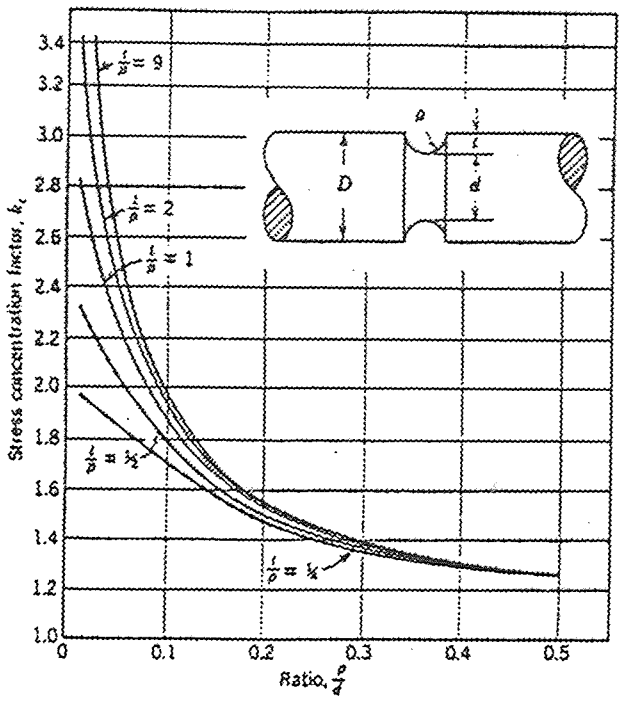

FIGURE 14 Theoretical stress concentration factors for semicircular grooves in cylindrical members subjected to bending, (62).

Nominal shearing stress = $\tau_0 = \tau_{max}/K_t$

τ_0 = 8.35 MPa

3.3.3 Stresses on the Carriage Pin

The carriage-pin allows the femoral component to fit into the tibial component. At the proximal end, the carriage pin bears the hinge-pin across its vertical axis, FIGURE 15. Distribution of force across the tibial bearing surfaces and the carriage-pin can be classified under three types (69)

(i) If the resultant force passes through the center of the knee, the forces are evenly distributed.

(ii) If the resultant force is shifted either to the medial or the lateral side, forces are still carried by the bearing surfaces but are unevenly distributed.

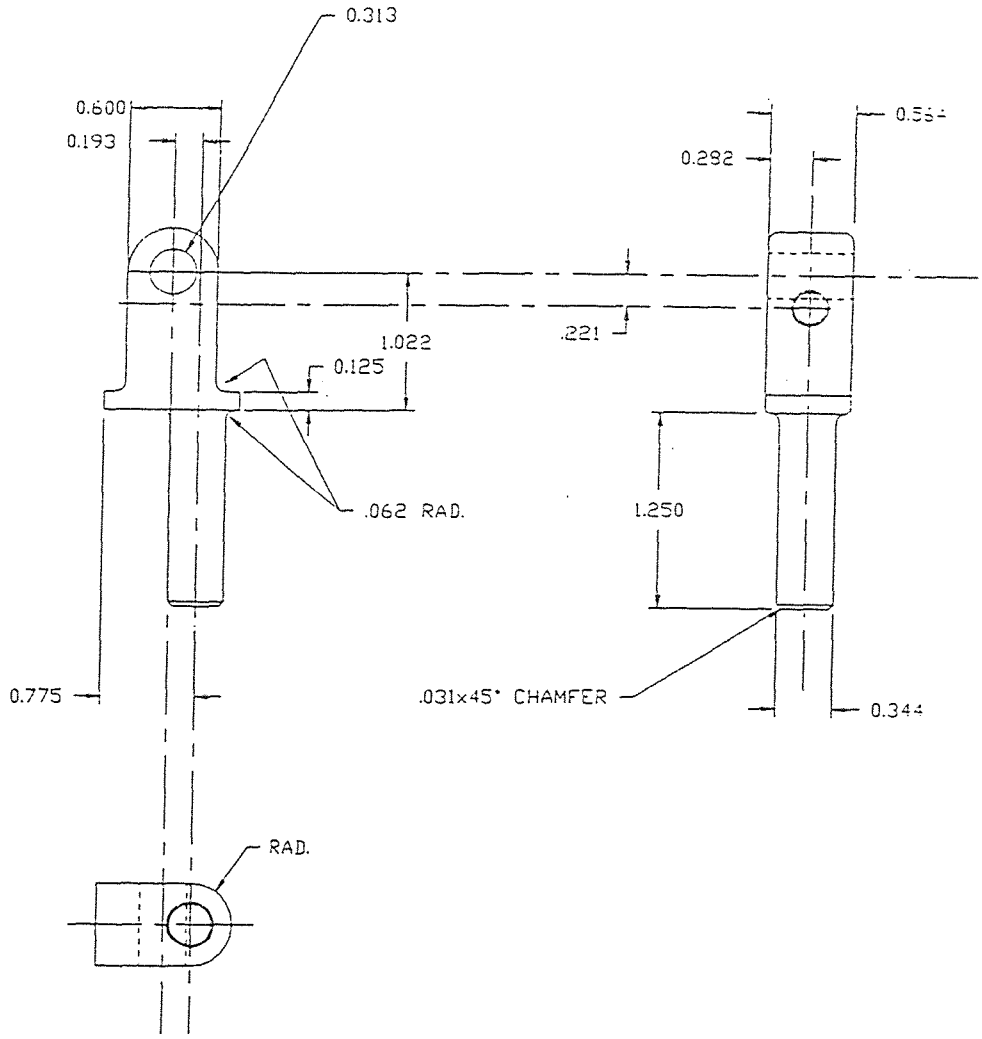

FIGURE 15 Carriage-pin component of the prosthesis. Units are in inches.

(iii) If the line of action is outside of the knee (either medial or lateral), the forces are carried on one side and the metal rod carries a moment equal to the force times distance.

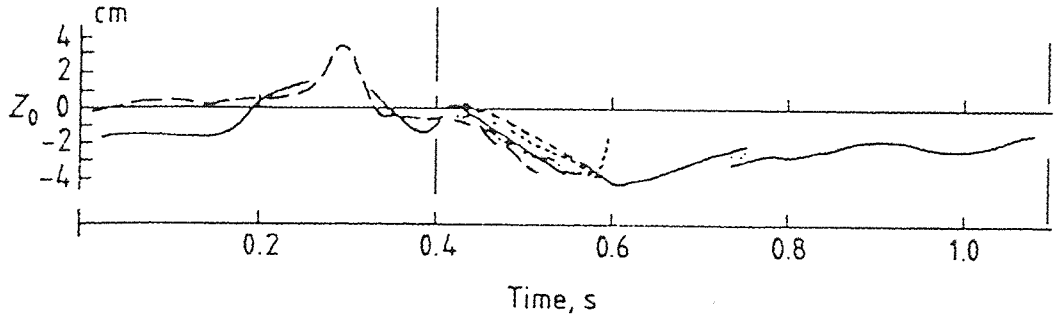

FIGURE 16 Point of application of the intercondylar force on the tibial plateau along the neutral axis, Z_0, (54).

In considering the potential areas of failure the worst case where the line of action of the axial force (Z_0) is 40 mm away from the center of the knee and the axial force on the knee is three times body weight FIGURE 16, (54).

Moment = M = (40-34.24) * 1063.64 N

M = 6.13 Nm

The value of 34.24 mm is found from the geometry of the condylar region of the distal femur, the distance from the center of the knee to either the lateral or medial side. Therefore, for the worst case where the carriage pin is rigidly supported in the tibial insert with the top of the stem carrying all the moment without support,

Diameter of the carriage pin = 8.6 mm

Bending stress = σ = M * Distance from the neutral y-axis

÷ moment of inertia

Bending stress = $\sigma = (6.13 * 4.3*10^{-3})/[(0.0043^{4}*\pi)/4]$

σ = 98.16 MPa

3.4 Material Properties

The accompanying table 5 provides a primary list of engineering properties of the materials used in the prosthesis design (10, 24). The standard values for the materials are compared to those from the previous analysis.

TABLE 5 Engineering properties of materials used in the design of the prosthesis

Material	Modulus of Elasticity (GPa)	Tensile Yield Strength (MPa)	Ultimate Tensile Strength (MPa)
Ti6Al4V	99	700	750
UHMWPe	0.8	16.8	24
Stainless Steel	193	900	1300

3.4.1 Trochanteric Attachment

Sanders *et al.* (58) conducted fatigue tests on the multifilament stainless steel cables and obtained a tensile stress of 579 MPa at 5352 ± 397 cycles. Codman Inc. also conducted fatigue studies on stainless steel cables. Using the given information and using Basquin's equation of $A = \sigma_r * L^B$; it is estimated that the cable either reaches its endurance limit of exceeds a life of more that 10^7 cycles. The maximum stress experienced on the cable are 51.30 MPa while running and an average of 20 MPa when walking.

3.4.2 Expanding Component Cross-Pin

The fatigue properties for Ti6Al4V were derived from technical reports (1) and are shown in FIGURE 17. The cross-pin and the valgus-varus attachment pin were analyzed to experience a shear load of about three times the body weight which is in the order of 1063.64 N (stress of 5.6 MPa). Fatigue properties are available for cycles up to 10^7 but *in situ* the prosthesis will have

experienced more cyclic loading than the limit. This is less than 5% of the maximum stress (275 MPa) when cyclically loaded to 10^7 cycles.

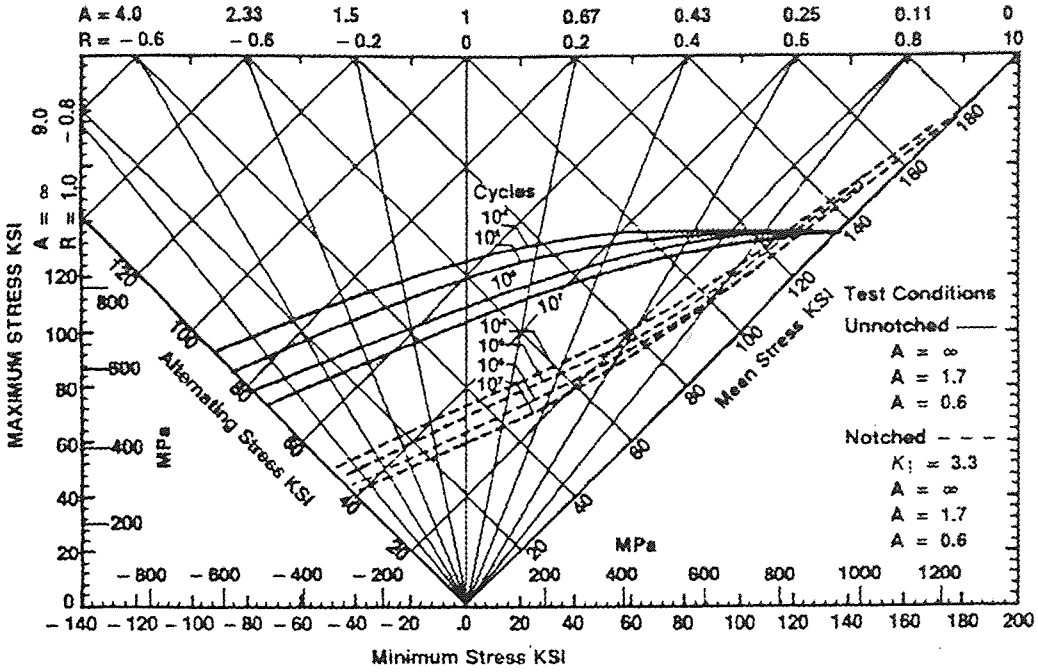

FIGURE 17 Typical constant-life fatigue diagram for annealed Ti6Al4V alloy (bar). Test frequency: 29 Hz, (1).

3.4.3 Hinge-Pin

The hinge-pin of the rotating hinge knee component experiences bending and shear of approximately 100 MPa and 11.23 MPa respectively when considered to be supported uniformly on UHMWPe. These are again less than the maximum stresses (275 MPa) required to fatigue the metal at 10^7 cycles.

3.4.4 Carriage-Pin

The carriage-pin, in the worst case scenario (54) undergoes a bending moment of 6.13 Nm and a bending stress of 98.16 MPa. On comparing with the fatigue data in (1), the metal is well under the safety limit of 275 MPa.

3.4.5 UHMWPe Wear

The prosthesis design includes the use of UHMWPe components. The hinge bushings and the tibial insert are the components that experience wear. According to the study done by Jacobson *et al.* (34), the titanium nitride coating improves the wear characteristics of the prosthesis. The studies included pin-on-disk tests under a contact stress of 1.95 GPa for 10 million cycles (approximated use of the articulating surface over a period of 10 years).

At seven million cycles the volumetric wear produced was 0.5 mm^3 and at ten million cycles the wear was 3.2 mm^3. Comparing the load conditions with that of the patient with a principal stress of 11 MPa, the amount of wear is going to be less over the same period of cycles.

3.4.6 Fatigue Characteristics of UHMWPe

Published data on the fatigue properties of polyethylene (26) show a maximum stress of 10 MPa at 10^7 cycles. The contact stress on the tibial insert experiences a principal stress of 11 MPa during the stance phase of gait. Due to this, it is always under cyclic loading. The contact stress exceeds the maximum stress and so the tibial insert will have to be considered for replacement due to fatigue failure.

3.4.7 Cold Flow of UHMWPe

Little (46) reported that he experimentally found that cold flow of UHMWPe happens at loads between 500-530 MPa. Cold flow is the creep behavior of polyethylene which results in local deformation that may be mistaken for wear. Neither the tibial plateau nor the hinge bushing experience such high stress and hence are within safe limits for cold flow.

3.5 Gait Analysis

The patient's gait was analyzed 13 months postoperatively at the Orthopaedic Engineering and Research Center, Helen Hayes Hospital, West Haverstraw, NY. The analysis was performed using a computer aided video-motion analysis system (VICON) with five infra-red motion cameras that recorded the trajectories of passive reflective markers placed on key anatomic sites on the lower extremities. Ground reaction forces were measured with force plates and the kinematic and kinetic data were analyzed on a VAX computer. The phasic activity of the muscle groups were recorded using surface electrodes and were correlated to the walking cycle using foot switches. The patient has adopted compensatory measures to deal with the postoperative muscular deficits in his lower extremity in the following ways:

(i) In order to reduce the resultant joint forces, the patient has developed an ipsilateral trunk tilt reducing the joint moments.

(ii) To compensate for the incomplete right hip extension the patient tilts the pelvis anteriorly.

(iii) Hip flexion is completed by the patient posteriorly tilting the pelvis and internally rotating the thigh for limb propulsion.

(iv) The patient's reduced knee extension is the result of weak quadriceps muscles resulting in a stiff knee gait (FIGURE 18).

A number of clinical recommendations were made based on the gait analysis including rehabilitation exercises focusing on proximal muscle

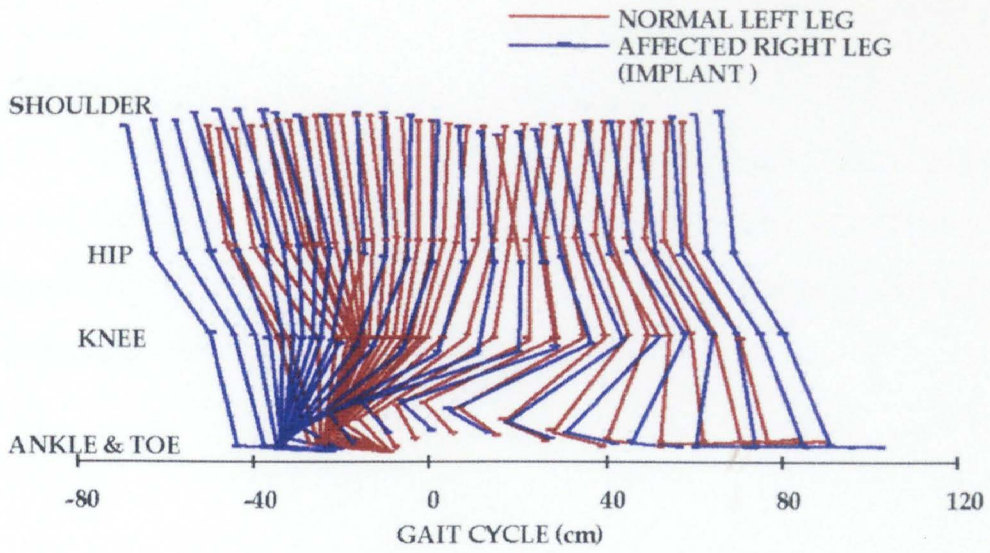

FIGURE 18 Stick figure of the patients gait highlighting the joint center data of the affected right limb (implant) and the normal left limb.

strengthening (FIGURE 19) and gait therapy addressing abnormal motion and control patterns. Further gait analyses are planned at six months intervals to assess changes due to growth and prosthesis lengthenings.

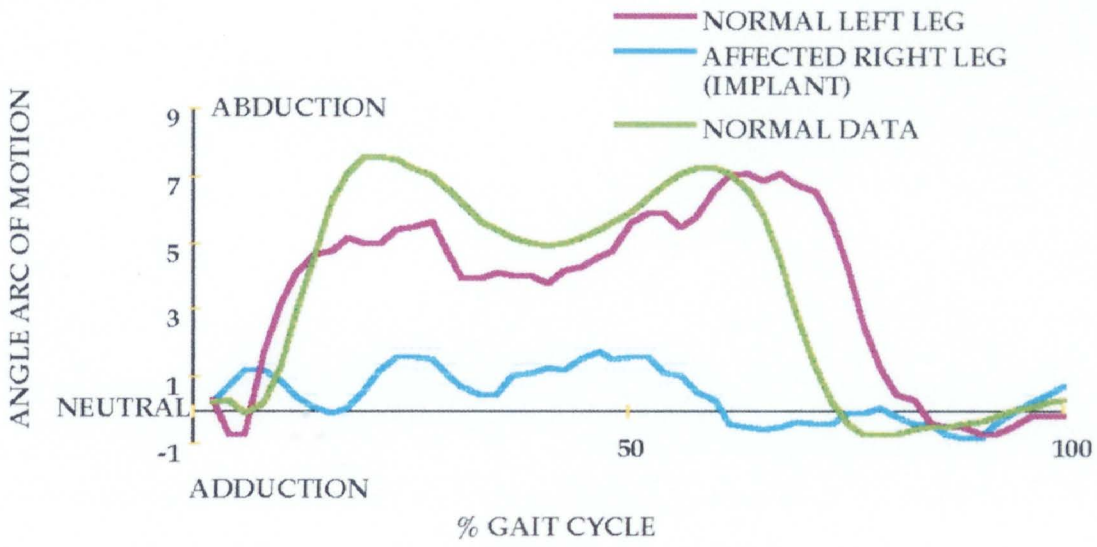

FIGURE 19 Proximal muscle weakness of the affected right leg is clearly evident due to reduced arc of motion.

3.6 Expansion Surgery

16 months postoperatively, the contralateral limb of the patient was found to be approximately 15.3 mm longer than the affected limb. An expansion surgery was done to compensate for this discrepancy. The prosthesis was expanded by one cross-pin hole corresponding to about 9 mm of lengthening. Postoperatively the patient is doing well.

4 CONCLUSIONS

This prosthesis was designed to address two problems; (i) limb growth, and (ii) femoral replacement. A novel expanding prosthesis was designed and theoretical analysis was conducted to determine stresses within various components.

The forces acting on the cables reconnecting the greater and lesser trochanter were determined for bipedal stance, single-legged stance, stance phase of gait, and running (0.5 MPa, 17 MPa, 23 MPa and 51 MPa respectively). These forces were then compared to the fatigue data on stainless steel cables. Using the given information and Basquin's equation of $A = \sigma_r * L^B$; it is estimated that the cable either reaches its endurance limit of exceeds a life of more that 10^7 cycles.

The expanding component cross-pin was analyzed to undergo loads of up to three times the body weight. Fatigue studies on Ti6Al4V show that the maximum stress required for failure is 275 MPa at 10^7 cycles. The cross-pin is not expected to fail in fatigue since the forces acting on it are considerably lower (less than 5%) than the maximum stress.

The cylindrical bearing surfaces between titanium alloy and UHMWPe experiences contact stresses of 11 MPa, which is greater than the calculated maximum stress that the UHMWPe would experience during fatigue loading. Due to these high stresses it is assumed that the polyethylene bearing component will need to be replaced at about 10^4 cycles. It should be noted that this value is based on a theoretical analysis and *in situ*, local deformation of the UHMWPe takes place reducing the contact stresses across the contact area. Also the maximum fatigue strength quoted was determined with cantilever bending and the value for compressive fatigue was not found. On analysis,

the UHMWPe surface experiences a compressive fatigue loading and not cantilever bending and hence the values obtained cannot be directly correlated with failure of the component

Rotating knee hinge-pin component was analyzed in bending and shear, the low stresses (100 MPa and 11 MPa respectively) on the pin would give a working life of more than 10^7 cycles.

The carriage-pin experiences a maximum bending stress of 98.16 MPa which is less than 50% of the maximum stress required for the titanium alloy to fail at 10^7 cycles.

Complete analysis was restricted to elementary theoretical assumptions. These assumptions include the fact that no growing phase was considered; dynamics of the patient were not dealt with; a fatigue limit of ten million cycles was used rather than the required one hundred million cycles; and the remodeling of the bone due to modified stresses was not been taken into consideration.

The patient was assumed to have regular physical activity but due to the age of the patient, this activity will exceed the normal range.

The gait analysis results have been studied and it was concluded that the patient has adopted various compensatory measures to deal with the postoperative muscular deficits in his right lower extremity.

At present, seventeen months postoperatively, the patient is ambulatory without any external support and does not complain of any pain. The patient's range of motion is within normal limits. One expansion surgery had been done to correct the limb length discrepancy and the patient is doing well.

REFERENCES

1. *Properties and Processing of Ti6Al4V*. In: TIMET, 1990.

2. Accardo, N.: Noiles Knee Replacement Procedure: A Six year Experience. *Orthopaedic Transactions*. 6:436-437; 1982.

3. Accardo, N.; Noiles, D.; Penna.; and Rudolph: Noiles Total Knee Replacement. *Orthop*. 2:37-45; 1979.

4. Anderson, M.; and Green, W.: Growth and Prediction of Growth in the Lower Extremities. *Clin. Orthop. Rel. Res*. (136):7-12; 1978.

5. Arden, G.; and Kamdar, B.: Complications of Arthroplasty of the knee. In: IMechE, ed. *Total Knee Replacements*. London: IMechE; 1974.

6. Attenborough, C.: The Attenborough Total Knee Replacement. *Journal of Bone and Joint Surgery*. 60B(3); Aug. 1978.

7. Bargar, W.; III, A. C.; and Amstutz, H.: Results with the Constrained Knee Prosthesis in Treating Severely disabled Patients and Patients with Failed Total Knee Replacements. *Journal of Bone and Joint Surgery*. 62A(4); June 1980.

8. Baumgart, R.; Betz, A.; and Schweiberer, L.: A Fully Implantable System for Prolonging Limbs and Shifting Segments. *International Biomechanics & Biomaterials Conference*. Italy, 1992.

9. Biehl, T.; Gredinger, R.; Thomas, W.; Hipp, E.; and Aigner, R.: The New-GT Custom made Knee Joint Prosthesis for Malignant Bone Tumors. In: Enneking W, ed. *Limb Salvage in Musculoskeletal Oncology*. New York: Churchill Livingstone; 1987: 599-604.

10. Black, J.: *Orthopaedic Biomaterials in Research and Practice*. New York: Churchill Livingstone; 1988.

11. Buechel, F.; and Pappas, M.: *New Jersey Knee Replacement system: Rationale and Review of 181 cases*. In: Biomedical Engineering corporation, 1983.

12. Buechel, F.; and Pappas, M.: New Jersey Low Contact Stress Knee replacement System. 10 year Evaluation of Meniscal Bearings. *Orthop. Clin. North Amer*. 20(2); April 1989.

13. Bernard, C; and Pellman, M.: A Review of Plasma Surface Modification Processes for Titanium Alloys. *19th Annual Meeting of the Society for Biomaterials.* Alabama, USA, 1992.

14. Dall, D.: Exposure of the Hip by Anterior Osteotomy of the Greater Trochanter: A modified anterolateral Approach. *Journal of Bone and Joint Surgery.* 68B(3); 1986.

15. Dall, D.; and Miles, A.: Re-attachment of the Greater Trochanter: The Use of the Trochanteric Grip System. *Journal of Bone and Joint Surgery.* 65B(1); 1983.

16. Davy, D.; Kotzar, G.; Brown, R.; Heiple, K.; Goldberg, V.; Jr., K. H.; Berilla, J.; and Burstein, A.: Telemetric Force Measurements Across the Hip After Total Arthroplasty. *Journal of Bone and Joint Surgery.* 70A(1); 1988.

17. Deburge, A.; Aubriot, J.; Genet, J.; and GUEPAR: Current status of a Hinge Prosthesis (Guepar). *Clin. Orthop. Rel. Res.* (145); 1979.

18. Deburge, A.; and GUEPAR: Guepar Hinge Prosthesis: Complications and results with Two year Follow-up. *Clin. Orthop. Rel. Res.* 120; Oct. 1976.

19. Eckardt, J.; Eilber, F.; Kabo, J.; and Mirra, J.: Kinematic Rotating Hinge Knee - Distal Femoral Replacement. In: Enneking W, ed. *Limb Salvage in Musculoskeletal Oncology.* New York: Churchill Livingstone; 1987.

20. Eckardt, J.; Matthews, J.; and Eilber, F.: Endoprosthetic Replacement after Bone Tumor Resection of the proximal Tibia. *Orthop. Clin. North Amer.* 22(1); Jan. 1991.

21. Endoh, H.; Seedholm, B.; and Takeda, T.: Mobility, Stability, and Stress in Artificial Knees. A comparative Study of Nine prostheses Representative of the Condylar Surface Replacement type. *Engineering in Medicine.* 7(2); 1978.

22. Engelbrecht, E.; Siegel, A.; Rottger, J.; and Buchholz, H.: Statistics of Total Knee Replacement: Partial and total Knee Replacement, Design St. George., A Review if a 4 year Observation. *Clin. Orthop. Rel. Res.* (120); Oct. 1976.

23. Finn, H.; Golden, D.; Kneisi, J.; and Simon, M.: The Finn Knee: Rotating Hinge Replacement of the Knee. Primary Report of New Design. In: brown K, ed. *Complications of Limb Salvage: Prevention, Management and Outcome. 6th International Symposium.* Montreal, Canada. ISOLS, Montreal, 1991.

24. Georgette, F.; and Sanders, T.: The Fatigue Resistance of Orthopaedic Wire and Cable Systems. *10th Annual Meeting of the Society for Biomaterials.* Washington D.C.: World Conference on Biomaterials, 1984.

25. Goel, V.; and Svensson, N.: Forces on the Pelvis. *Journal of Biomechanics.* 10:195-200; 1977.

26. Hertzberg, R.; and Manson, J.: *Fatigue of Engineering Plastic..* New York: Academic Press; 1980.

27. Hodge, W.; and Chandler, H.: Unicompartmental Knee Replacement: A Comparison of Constrained and Unconstrained Designs. *Journal of Bone and Joint Surgery.* 74A(6); July 1992.

28. Holt Jr., E.: Use of the Noiles Knee Prosthesis in Advanced Diseases. *Orthopaedic transactions.* 5:467; 1981.

29. Horowitz, S.; Lane, J.; Otis, J.; and Healy, J.: Prosthetic Arthroplasty of the Knee after Resection of a Sarcoma in the Proximal end of the Tibia. *Journal of Bone and Joint Surgery.* 73A(2); Feb. 1991.

30. Hui, F.; and Jr., R. F.: Hinged Total knee Arthroplasty. *Journal of Bone and Joint Surgery.* 62A(4); June 1980.

31. Huson, A.; Spoor, C.; and Verbout, A.: A Model of the Human knee, derived from Kinematic Principles and its Relevance for Endoprosthesis Design. *Acta Morphol. Neerl. Scand.* 27:45-62; 1989.

32. Inman, V.: Functional Aspects of the Abductor Muscles of the Hip. *Journal of Bone and Joint Surgery.* 29(3); 1947.

33. Insall, J.; Ranawat, C.; Aglietti, P.; and Shine, J.: A Comparison of Four Models of Total Knee Replacement Prostheses. *Journal of Bone and Joint Surgery.* 58A(6); Sept. 1976.

34. Jacobson, D.: *Wear and Friction of TiN on UHMWPe for Evaluation of Use in Articulating Orthopaedic Applications* [Master's Degree]. New Jersey Institute of Technology, 1992.

35. Kagan, A.: Mechanical causes of Loosening in Knee Joint Replacements. *Journal of Biomechanics*. 10:387-391; 1977.

36. Kaufer, H.; and Matthews, L.: Sphreocentric Knee Arthroplasty. *Clin. Orthop. Rel. Res.* (145); 1979.

37. Keanan, S.; and Lewis, M.: Limb Salvage in Pediatric Surgery: The Use of the Expanding prosthesis. *Orthop. Clin. North Amer.* 22(1); Jan. 1991.

38. Keanen, S.; Bloom, N.; and Lewis, M.: Limb Sparing Surgery in Skeletally Immature Patients with Osteosarcoma. *Clin. Orthop. Rel. Res.* (270); Sept. 1991.

39. Kenesi, C.: The Caviar Madreporic Knee Prosthesis. *Clin. Orthop. Rel. Res.* (145); 1979.

40. Kester, M.; Cook, S.; Harding, A.; Roddriguez, R.; and Pipkin, C.: An Evaluation of the Mechanical Failure Modalities of a Rotating Hinge Knee Prosthesis. *Clin. Orthop. Rel. Res.* (228); March 1988.

41. Kneisl, J.; Finn, H.; and Simmons, M.: Mobil Knee Reconstructions after Resection of Malignant Tumors of the Distal Femur. *Orthop. Clin. North Amer.* 22(1); Jan. 1991.

42. Kotz, R.; and Ritschl, P.: Modular Replacement of femur and Tibia. In: Brown K, ed. *Complications of Limb Salvage: Prevention, Management and Outcome, 6th International Symposium.* Montreal, Canada: ISOLS, Montreal, 1991.

43. Lettin, A.; Blackburne, D.; and Setal, J.: The Stanmore Hinged Knee Arthroplasty. *Journal of Bone and Joint Surgery*. 60B(8); 1978.

44. LeVeau, B.: *Williams & Lissner: Biomechanics of Human Motion.* Philadelphia: WB Saunders Company; 1977.

45. Lewis, M.: *Bone Tumor Surgery: Limb Sparing Techniques.* Philadelphia: J. B. Lippincott; 1988.

46. Little, E.: Compressive Creep Behavior of Irradiated Ultra High Molecular Weight Polyethylene at 37°C. *Engineering in Medicine.*; 1985.

47. Marcove, R.; and Khafagy, M.: Total Femur and Knee replacement using a Metallic Prosthesis. *Clinical Bulletin* 1977

48. Marcove, R.; Lewis, M.; Rosen, G.; and Hoves, A.: Total Femur and Total Knee Replacement. *Clin. Orthop. Rel. Res.* (126); Aug. 1977.

49. May, W.: Relative Isometric Force of the Hip Abductor and Adductor Muscles. *Physical Therapy.* 48(8); 1976.

50. McLeish, R.; and Charnley, J.: Abduction Forces in the One Legged Stance. *Journal of Biomechanics.* 3:191-209; 1970.

51. Murase, K.; Crownshield, R.; Pederson, D.; and Chang, T.: An Analysis of Tibial Component Design in Total knee Replacement. *Journal of Biomechanics.* 16(1):13-22; 1983.

52. Murray, D.; Wilde, A.; Weener, F.; and Foster, D.: Herbert Total Knee Prosthesis. *Journal of Bone and Joint Surgery.* 59A(8); Dec. 1977.

53. Nerubay, J.; Katznelson, A.; Rubinstein, Z.; Tichler, T.; and Bubis, J.: Total Femoral Replacement. In: Brown K, ed. *Complications of Limb Salvage: Prevention, Management and Outcome. 6th International Symposium.* Montreal, Canada. ISOLS, Montreal, 1991.

54. Nissan, M.: The Use of a Permutation Approach in the Solution of Joint Mechanics: The Knee. *Engineering in Medicine.* 10(1); 1981.

55. Pappas, M.; Makris, G.; and Buechel, F.: *Contact Stress in Metal-Plastic Knee Replacements: A Theoretical and Experimental Study.* In: Biomedical Engineering Trust, NJ, 1986.

56. Popov, E.: *Introduction to Mechanics of Solids.* New Jersey: Prentice-Hall, Inc., Englewood; 1983.

57. Present, D.; and Kuschner, S.: Total Femur Replacement: A Case Report with 35 year Follow-up Study. *Clin. Orthop. Rel. Res.* (251); Feb. 1990.

58. Sanders, T.; Treharne, R.; Baswell, I.; and Oh, I.: Development of a New Orthopaedic Wire Fatigue Tester. *J. Biomed. Mat. Res.* 17:587-96; 1983.

59. Scales, J.; and Sneath, R.: The Extending Prosthesis. In: Coombs R, Friedlander G, ed. *Bone Tumor Management.* Butterworth; 1987.

60. Scales, J.; Sneath, R.; and Wright, K.: Design and Clinical Use of Extending Prostheses. In: Enniking W, ed. *Limb Salvage in Musculoskeletal Oncology.* New York: Churchill Livingstone; 1987.

61. Schlepckow, P.: Three Dimensional Kinematics of Total knee Replacement System. *Arch.Orthop.Trauma.Surg.* 111:204-209; 1992.

62. Seely, F.; and Smith, J.: *Advanced Mechanics of Materials.* New York, New York: Wiley & Sons, Inc.; 1958.

63. Seireg, A.; and Arvikar, R.: The Prediction of Muscular Load Sharing and Joint Forces in the Lower Extremities During Walking. *Journal of Biomechanics.* 8:89-102; 1975.

64. Sheehan, J.: Arthroplasty of the Knee. *Clin. Orthop. Rel. Res.* (145); 1979.

65. Shindell, R.; Neuman, R.; Connolly, J.; and Jardon, O.: Evaluation of Noiles Hinged Knee Prosthesis: A 5 year Study of 17 Cases. *Journal of Bone and Joint Surgery.* 68A(4); April 1986.

66. Sim, F.; Beauchamp, C.; and Chao, E.: Reconstruction of Musculoskeletal defects about the Knee for Tumor. *Clin. Orthop. Rel. Res.* (221); Aug. 1987.

67. Steinbrink, K.; Englebrect, E.; and Fenclon, G.: The Total Femoral Prosthesis: A Preliminary Report. *Journal of Bone and Joint Surgery.* 63B(305); 1982.

68. Verkerke, G.: *Design and Testing of an Extendible Modular Endoprosthesis System for Bone Tumor Management in the Leg* [Ph.D. Degree]. University of Twente, Netherlands, Dec. 1989.

69. Walker, P.; Emerson, R.; Potter, T.; Scott, R.; Thomas, W.; and Turner, R.: The Kinematic Rotating Hinge: Biomechanics and Clinical Application. *Orthopaedic Clinics of North America.* 13(1); Jan. 1982.

70. Wilson, F.; and Venters, G.: Results of Knee Replacement with the Walldius Prosthesis: An Interim Report. *Clin. Orthop. Rel. Res.* (120); Oct. 1976.

71. Wright, K.: Bioengineering Aspects of Prosthetic Design. In: Coombs R, Friedlander R, ed. *Bone Tumor Management.* Butterworth; 1987.